BIOCHEMISTRY
including biophysical chemistry & molecular biology

Article

pubs.acs.org/biochemistry

Atomic-Resolution Structures of Horse Liver Alcohol Dehydrogenase with NAD$^+$ and Fluoroalcohols Define Strained Michaelis Complexes

Bryce V. Plapp*[,†] and S. Ramaswamy[†,‡]

[†]Department of Biochemistry, The University of Iowa, Iowa City, Iowa 52242, United States

[‡]Institute for Stem Cell Biology and Regenerative Medicine (inSTEM), National Center for Biological Sciences, GKVK Post, Bellary Road, Bangalore 560065, India

ABSTRACT: Structures of horse liver alcohol dehydrogenase complexed with NAD$^+$ and unreactive substrate analogues, 2,2,2-trifluoroethanol or 2,3,4,5,6-pentafluorobenzyl alcohol, were determined at 100 K at 1.12 or 1.14 Å resolution, providing estimates of atomic positions with overall errors of ~0.02 Å, the geometry of ligand binding, descriptions of alternative conformations of amino acid residues and waters, and evidence of a strained nicotinamide ring. The four independent subunits from the two homodimeric structures differ only slightly in the peptide backbone conformation. Alternative conformations for amino acid side chains were identified for 50 of the 748 residues in each complex, and Leu-57 and Leu-116 adopt different conformations to accommodate the different alcohols at the active site. Each fluoroalcohol occupies one position, and the fluorines of the alcohols are well-resolved. These structures closely resemble the expected Michaelis complexes with the *pro-R* hydrogens of the methylene carbons of the alcohols directed toward the *re* face of C4N of the nicotinamide rings with a C−C distance of 3.40 Å. The oxygens of the alcohols are ligated to the catalytic zinc at a distance expected for a zinc alkoxide (1.96 Å) and participate in a low-barrier hydrogen bond (2.52 Å) with the hydroxyl group of Ser-48 in a proton relay system. As determined by X-ray refinement with no restraints on bond distances and planarity, the nicotinamide rings in the two complexes are slightly puckered (quasi-boat conformation, with torsion angles of 5.9° for C4N and 4.8° for N1N relative to the plane of the other atoms) and have bond distances that are somewhat different compared to those found for NAD(P)$^+$. It appears that the nicotinamide ring is strained toward the transition state on the path to alcohol oxidation.

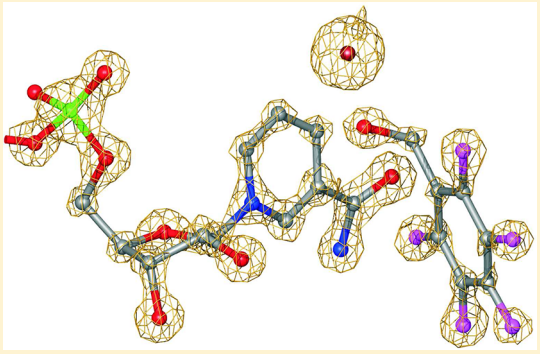

Horse liver alcohol dehydrogenase (ADH, EC 1.1.1.1) is a very well-studied enzyme.[1] The kinetics and catalytic mechanism have been described previously.[2] Three-dimensional structures have been determined for a variety of complexes with native and mutated enzymes.[3,4] ADH is the first enzyme for which a conformational change involving rotation of domains upon binding a substrate was described;[5] this conformational change is intimately related to catalysis.[6] Kinetic isotope effects provide evidence of quantum mechanical hydrogen tunneling during catalysis,[7] and temperature-independent isotope effects are consistent with a role for vibrationally assisted tunneling.[8−11] Computational studies, based on three-dimensional structures of ADH, have addressed the energetics of proton and hydride transfer steps and the roles of protein motion in catalysis.[12−18] Nevertheless, the connection between protein dynamics and tunneling has not yet been established.[19] Furthermore, some atomic-resolution X-ray studies of ADH raise questions about the chemistry of interconversion of ternary complexes during catalysis.[20,21]

Atomic-resolution structures[22] provide a wealth of detail that is critical for understanding enzyme function. For such studies, it is important to crystallize the enzyme with the actual substrates or ligands that are sterically and chemically similar to the substrates. For alcohol dehydrogenase, complexes with NAD$^+$ and fluoroalcohols are especially informative because the fluorines are sterically similar to hydrogens, are readily visible in electron density maps, and produce an unreactive substrate analogue because of electron withdrawal, so that the nicotinamide ring should remain oxidized. The alcohols chosen for this study, 2,3,4,5,6-pentafluorobenzyl alcohol (PFB) and 2,2,2-trifluoroethanol (TFE), are potent competitive inhibitors of alcohol oxidation by ADH (K_i values of 0.52 and 8.4 μM, respectively). A structure with the wild-type enzyme complexed with PFB was previously determined at 2.1 Å resolution at 4 °C.[23] PFB is a good analogue of benzyl alcohol, a good substrate that has been used extensively for kinetic studies and evaluation of quantum mechanical tunneling. TFE is an analogue of the natural substrate, ethanol, and no high-resolution structure with the wild-type enzyme has been reported, although there are moderate-resolution structures with mutated ADHs that are centerpieces for understanding the requirements for hydrogen tunneling.[19] With cryocrystallog-

Received: March 23, 2012
Revised: April 24, 2012
Published: April 24, 2012

raphy and synchrotron radiation, the desired atomic-resolution structures could be determined.

EXPERIMENTAL PROCEDURES

Crystallization. Wild-type (natural) crystalline horse liver alcohol dehydrogenase (EE isoenzyme) and LiNAD$^+$ were purchased from Roche Molecular Biochemicals. The fluoroalcohols (98−99%) were purchased from Aldrich and used without further purification. 2-Methyl-2,4-pentanediol was obtained from Kodak and treated with activated charcoal before being used. The crystals of wild-type ADH complexed with NAD$^+$ and the fluoroalcohols were prepared as described by the general procedure used previously.[23] The enzyme was first recrystallized from 10 mM sodium phosphate buffer (pH 7.0) at 4 °C with 10% ethanol; the crystals were redissolved in buffer with some added KCl, and the solution was dialyzed extensively against 50 mM ammonium *N*-[tris(hydroxymethyl)-methyl]-2-aminoethanesulfonate buffer and 0.25 mM EDTA (pH 6.7) (measured at 25 °C and pH 7.0 and at °C). The solution was clarified by centrifugation. Approximately 1 mL of 10 mg/mL (A_{280} = 0.455 cm^{-1} for 1 mg/mL) enzyme was dialyzed in washed $^1/_4$ in. diameter tubing at 4 °C against 10 mL of the same buffer with 1 mM NAD$^+$ and 10 mM pentafluorobenzyl alcohol or 100 mM trifluoroethanol for ∼1 h, and then the concentration of 2-methyl-2,4-pentanediol was increased by dialysis over some days to 12% when crystals formed. After that, the concentration of the diol was increased slowly to a final value of 25%, which was sufficient for cryoprotection at 100 K.

X-ray Crystallography. The crystals (∼0.3−0.4 mm thick) for both complexes were mounted on fiber loops (Hampton Research) and flash-cooled by being plunged into liquid N_2. X-ray data were collected at 100 K. The data for the pentafluorobenzyl alcohol complex were collected March 9, 2006, on the GM/CA-CAT 23ID beamline with a MAR300CCD detector at the Advanced Photon Source with an X-ray wavelength of 0.9537 Å with a 0.025 mm × 0.075 mm beam and a 133 mm distance with 8 s exposures and 0.2° oscillations over 360° total and then for a low-resolution pass at 300 mm with 2 s exposures with 0.2° oscillations over 360° total. The data for the trifluoroethanol complex were collected June 24, 2009, on the SBC 19ID beamline with an ADSC315r Quantum detector at APS with an X-ray wavelength at 0.9184 Å with a 0.05 mm × 0.05 mm beam and a 130 mm distance, with 4 s exposures with 0.5° oscillations for 760 images covering 380° total. Data were processed with d*TREK.[24] Both structures were determined by molecular replacement using the coordinates for the refined wild-type ADH−NAD$^+$−2,3,4,5,6-pentafluorobenzyl alcohol complex [Protein Data Bank (PDB) entry 1HLD] as a model.[23] The structures were refined by cycles of restrained refinement with REFMAC5[25] and model building with O.[26] Model bias was avoided during the initial refinement by not including the fluoroalcohol in the model, and omit maps were used where structural features were in doubt. Initially, the nicotinamide ring in the NAD$^+$ molecule dictionary was set to be planar, but as a test of the identity of the coenzyme, the monomer dictionary used by REFMAC was modified to remove the restraints on planarity and relax the restraints on bond distances (from 0.02 to 0.10 Å) for the nicotinamide ring. This modified coenzyme is named NAJ in our coordinate files to distinguish it from NAD (with tight restraints) listed in other structures. SHELXL[27] was also used for refinement with no restraints for the coenzyme. After rounds of blocked, diagonal least-squares refinement, a blocked, full-matrix refinement was used to determine bond distances and their errors for important structural features.

During the early stages of refinement, hydrogens were included in riding positions, and isotropic temperature factors were refined. The hydrogens contribute to scattering, decreasing the *R* values (by ∼1%), but not sufficiently to be refined in a manner independent of the parent atom. Hydrogens in methyl, amino, and hydroxyl groups, where the torsion angle is not known, were given zero occupancy. Alternative conformations of amino acids and waters were assigned on the basis of indisputable visual evidence: divergent electron densities at the +1σ level above the average in $2|F_o| - |F_c|$ maps, divergent lobes, and consistent plus/minus densities at +3.5/−3.5σ in $|F_o| - |F_c|$ maps. Occupancies were adjusted to make the temperature factors similar for the alternative positions. An arbitrary cutoff for *B* values for water molecules was not applied, but waters were included when there was density above +1σ in $2|F_o| - |F_c|$ maps and the distances to other atoms were compatible with hydrogen bonds. Single waters were fit in most cases, but bilobate ("dumbbell") densities were fit with two alternative atoms when the distances were between ∼1.6 and ∼2.4 Å. Some waters were placed in ellipsoidal densities, which were assumed to be characterized by anisotropic refinement. Extensive clusters of waters were observed. Partial waters were included to fit alternative conformations of amino acid residues. In the final stages, refinement with anisotropic temperature factors for all atoms with a restraint of 10 for sphericity was used. The final models were well-described by the electron density maps; however, side chains for some residues on the surface of the protein (such as lysine and glutamic acid residues) were not completely within the density, and many peaks of density, probably because of additional water or methylpentanediol molecules, were not modeled because of a lack of contacts with the protein. The amino-terminal acetyl groups found for the enzyme isolated from horse liver[1] were not modeled, for lack of density. The structures were checked with PROCHECK.[28] All residues had favored or allowed backbone conformational angles, except that Cys-174 residues (ligated to the catalytic zincs) were in the generously allowed region. EXCEL was used for statistical analyses.

RESULTS AND DISCUSSION

Refinement and Model Building. Table 1 summarizes the X-ray data collection and refinement. The homodimeric molecule in the asymmetric unit has a total of 748 amino acid residues, four zinc atoms, two NAD$^+$ molecules, four methylpentanediols, two fluoroalcohols, and 1040 waters (in the complex with pentafluorobenzyl alcohol) or 1025 waters (in the complex with trifluoroethanol). Because of the alternative conformations, the number of fitted atoms is larger than the actual number in the structures.

The asymmetric unit is a dimer, consisting of two identical chemical subunits, but differing slightly in conformation. The structures of the complexes with PFB and TFE are essentially identical, superimposing all α-carbons with an rmsd of 0.09 Å. Superpositioning only the coenzyme binding domains (residues 176−318) of subunit A onto subunit B for the structure with pentafluorobenzyl alcohol gives an rmsd of 0.08 Å, whereas superpositioning of all residues is accomplished with an rmsd of 0.17 Å. The α-carbons of the superpositioned residues are almost identical, suggesting that the conformations of both

dx.doi.org/10.1021/bi300378n | *Biochemistry* 2012, 51, 4035−4048

Table 1. X-ray Data and Refinement Statistics for Horse Liver Alcohol Dehydrogenase Complexed with NAD$^+$ and Fluoroalcohols

	2,3,4,5,6-pentafluorobenzyl alcohol	2,2,2-trifluoroethanol
PDB entry	4DWV	4DXH
space group	P_1	P_1
no. of homodimeric molecules per unit cell	1	1
cell dimensions (Å)	44.29, 51.44, 92.49	44.25, 51.16, 92.53
cell angles (deg)	91.72, 103.1, 110.1	91.91, 103.0, 109.9
resolution range (Å)	20.0−1.14	20−1.12
no. of measured reflections (total, unique)	1203625, 253394	1073887, 267668
completeness (%) (outer shell)	93.7 (84.5)	94.2 (91.4)
R_{meas} (%) (outer shell)[a]	6.5 (30.8)	5.4 (42.2)
mean $\langle I\rangle/\sigma\langle I\rangle$ (outer shell)	12.9 (3.2)	9.7 (2.1)
R_{value}, R_{free}, test (%)[b]	12.4, 14.4, 1.0	12.7, 14.7, 0.5
mean B value (Å^2) (Wilson, REFMAC)	11.4, 14.9	9.6, 13.3
rsmd for bond distances[c] (Å)	0.013	0.011
rmsd for bond angles[c] (deg)	1.67	1.64
estimated error in coordinates (Å)	0.020	0.019
no. of atoms fit	6996	6973

[a] $R_{meas} = R_{rim}$ (redundancy-independent merging).[24] [b] $R = (\sum|F_o - kF_c|)/\sum|F_o|$, where k is a scale factor. R_{free} was calculated with the indicated percentage of reflections not used in the refinement.[88] [c] Root-mean-square deviations from ideal geometry.

subunits are very similar, but subunit B has a slightly more open conformation, giving rise to differences of up to 1 Å in the catalytic domain as compared to subunit A. The similarity in the subunits suggests that both active sites can be catalytically active and provides no evidence of cooperativity in catalysis.

The structure of ADH crystallized with NAD$^+$ and PFB previously reported at a resolution of 2.1 Å, determined at 4 °C,[23] and our structure superimpose using the coenzyme binding domains (residues 176−318) with an rmsd of 0.31 Å (0.37 for all α-carbons), but there is a small expansion of ∼0.7 Å in overall size at 177 °C. Previous studies that compared a series of structures of other proteins determined from 80−98 to 295−320 K also noted an expansion.[29−31] Most features are the same in both ADH structures, but some side chains have somewhat different positions. The additional data (250801 unique reflections compared to 37512) lead to a greatly improved structure, with many alternative conformations and more accurate estimates of noncovalent bond distances and anisotropic atomic displacement parameters. A structure of horse liver ADH with the A317C substitution (located near the carboxyamido group of the nicotinamide ring) was determined at 1.2 Å resolution and is almost identical to our structure (PDB entry 3OQ6).[32] This study analyzes the details of the atomic-resolution structures.

Active Site Architecture. The X-ray data provided electron density maps at atomic resolution. Figure 1 shows the binding of the NAD$^+$ and fluoroalcohols in maps that are contoured to show how the electron density envelopes grow in size with an increasing atomic number. The positions of the atoms are well-defined, and the fluorine atoms stand out. The

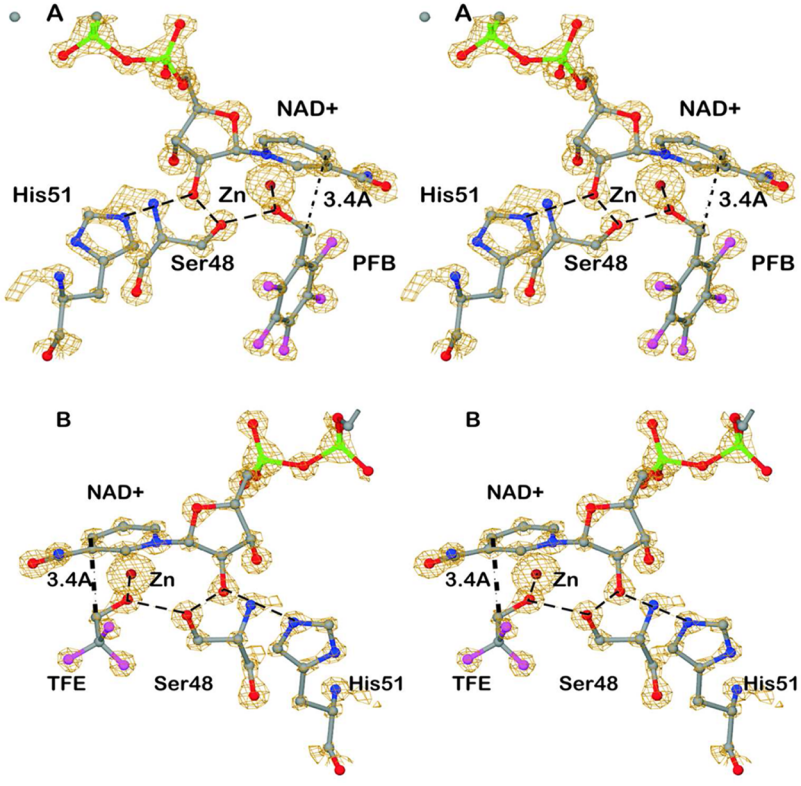

Figure 1. Electron density maps for complexes of ADH with NAD$^+$ and the fluoroalcohols. Interactions in the proton relay system are shown with dashed lines. The dotted line with the 3.4 Å label shows the distance between C4N of the nicotinamide ring and the methylene carbon of the alcohol. The stereoviews are rotated ∼180° to allow different views. (A) Binding of pentafluorobenzyl alcohol. The electron density is ∼4σ above the mean. (B) Binding of trifluoroethanol. The electron density is ∼4.9σ above the mean.

dx.doi.org/10.1021/bi300378n | *Biochemistry* 2012, 51, 4035−4048

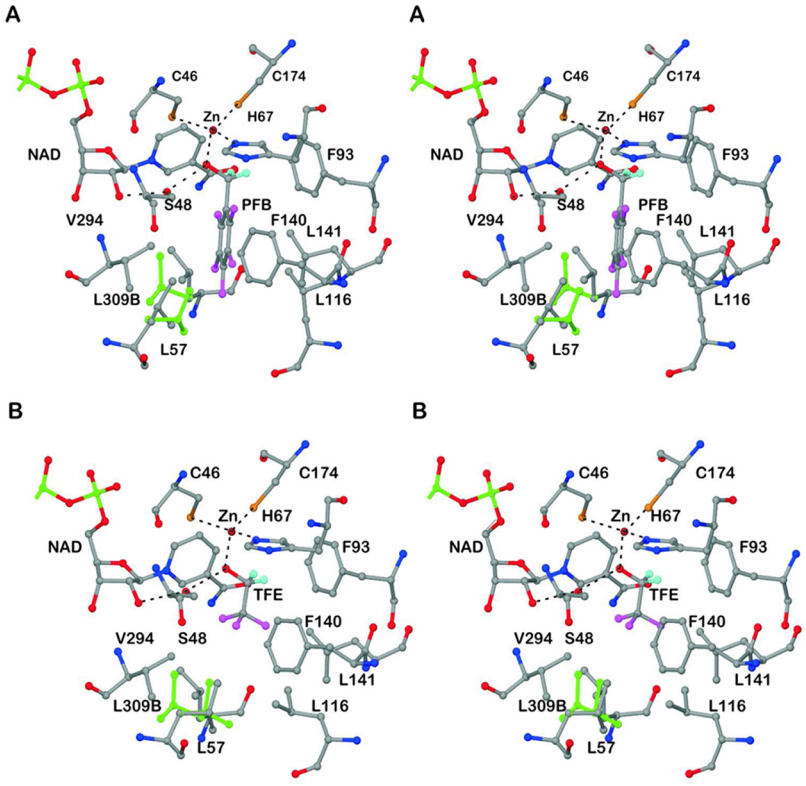

Figure 2. Interactions of alcohols with active site residues. The coordination of the catalytic zinc ion and the hydrogen bonds of the alcohol in the proton relay system are shown as dotted lines. The riding hydrogens of the methylene carbons are colored cyan, and the other atoms have the usual atomic coloring, except that the alternative conformations of the side chains of Leu-57 and Leu-309B (other subunit) are colored green. Note that the conformations of Leu-57 and Leu-116 differ in the two structures: (A) pentafluorobenzyl alcohol and (B) trifluoroethanol.

plane of the pentafluorobenzyl group is clear. The trifluoromethyl group has one position, suggesting a lack of free rotation about the C1−C2 bond. In each structure, the hydrogen-bonded network connecting the oxygen of the alcohol to His-51, which can act as the base in catalysis, is shown with dashed lines.[23,33,34] The distance between C4N of the nicotinamide ring and the methylene carbon of the alcohol is 3.4 Å in all four subunits, illustrating a ground-state complex that mimics the expected Michaelis complex.

Figure 2 illustrates the interactions of the two different fluoroalcohols in the substrate binding sites. The hydrogen atoms riding on the methylene carbons are included, to indicate that the *pro-R* hydrogen is directed toward the position expected for direct transfer of hydride to C4N (*re* face) of the nicotinamide ring.[35] The binding site is hydrophobic, consistent with the observation that this enzyme is very selective for nonpolar, primary alcohols. Ethanol is a major natural substrate, but longer chain alcohols, benzyl alcohols, and some secondary alcohols are also good substrates.[36] The conformations of amino acid residues in the binding site are adaptable, allowing different inhibitors to bind.[37,38] In the structures with the fluoroalcohols, residues Leu-57 and Leu-116 in the substrate binding pocket adopt different conformations (Figure 2), apparently optimizing hydrophobic interactions. The atomic resolution provides a more complete picture, as Leu-309 (from the other subunit) has alternative conformations in the structures with both alcohols and Leu-A57 has different and also alternative conformations in the structures with PFB and TFE. Leu-B57 and leucine residues A116 and B116 have different, but single, conformations in the structures with PFB and TFE; the alternative position for Leu-116 in the structure with TFE makes a cavity that accommodates a water that is hydrogen bonded to the carbonyl oxygen of Phe-93. (However, no water molecules are near the zinc or close to the nicotinamide ring.) Leu-309 has alternative conformations in both active sites of the two structures. The differing conformations represent energetically accessible states that can affect substrate specificity and the dynamics that lead to catalysis.

Because the van der Waals radii for H and F are similar (1.30−1.38 and 1.20 Å, respectively[39,40]), the fluoroalcohols are expected to be good steric analogues of the corresponding substrates, but the electronegative fluorines may also participate in weak C−H···F hydrogen bonds and affect binding.[41,42] The pentafluorobenzyl group binds in one position, and its rotation would be hindered by steric interactions with Leu-57, Leu-116, and Ser-48. Its position might also be stabilized by the weak interactions (3.2−3.3 Å F−C distance) of F4 and F5 with the CD1 and CD2 methyl groups of Leu-57 and of F6 with the CB methylene of Ser-48. Trifluoroethanol binds with a staggered conformation of the O relative to the fluorines, and the fluorines are ∼3.2 Å from the carbons of CE1 of Phe-93, the CG2 methyl group of Val-294, and CB of Ser-48. A 60° rotation of the trifluoromethyl group produces an eclipsed conformation, and the contact with Phe-93 is lost. These structures may offer some evidence of weak interactions between the fluorines and the protein.

The enzyme catalyzes the transfer of the *pro-R* hydrogen of ethanol, and the structure with trifluoroethanol provides a basis for explaining this stereospecificity. If the methyl group is rotated about the torsion angle for the oxygen and the methylene C (note this C is labeled as C2 in the PDB file) so

dx.doi.org/10.1021/bi300378n | *Biochemistry* 2012, 51, 4035−4048

Table 2. Alternative Amino Acid Conformations and Associated Partial Waters[a]

Arg	B120[b]
Asp	A161, AB273, AB252
Cys	A46,[c] AB282
Gln	A251 (A880, A1029), B251 (B746, B819), A299 (A700, A831, A1028, MRD A379), B299 (B864)
Glu	A107 (C═O, A729), B107 (C═O, B741), B167, A239 (A998), B239 (B930), AB252, A256 (A724, A901, B793), B256 (B812), B353 (B703), B366 (side chain and C═O, B690)
His	A138 (A829, A914[c])
Leu	A57, A61, AB309
Lys	A39, A185,[b] AB188, B212 (B778), A228 (A664), B228 (B907), AB247 (C═O), B315, AB330, A338, B338[c]
Met	AB40; AB336
Ser	A117, AB280, AB302
Val	AB184
waters (alternative, doubled)	A488, A514, A517, A615, A623, A646, A664 (by A228 Lys), A729 (by A107), A764, A857,[b] A862, A880 (by A251), A915, A926, A958, A980, A986, B444, B544, B630, B762, B774, B775, B876, B904, B907 (by B228 Lys), B909, B910, B911, B912, B927[b]

[a]Amino acid residues are numbered from 1 to 374 and waters from 401 upward in subunits A and B. AB signifies both subunits. Associated partial water molecules are given in parentheses. [b]Only in the TFE structure. [c]Only in the PFB structure.

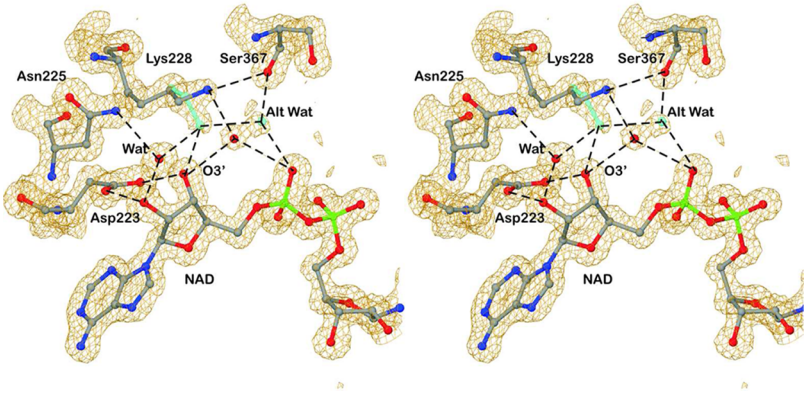

Figure 3. Alternative conformation for Lys-228 and its accompanying water. The green stick model and water represent the alternative positions. Hydrogen bonds are represented by dashed lines. The electron density map is contoured ~1σ above the mean.

that the *pro-S* hydrogen would point toward C4N of the nicotinamide ring, the methyl group would clash with the benzene ring of Phe-93. However, the reaction may be only highly stereoselective, as ~10% of the *pro-S* hydrogen from 1-octanol can be transferred.[43] This lack of specificity is an indication of structural flexibility and is also consistent with the observation that 2-propanol is a (poor) substrate.

Alternative Conformations. Fitting alternative conformations in structures determined by X-ray crystallography is required to obtain the best structures (lowest *R* factors and *B* factors), to identify potential chemical heterogeneity, and to describe conformational flexibility that reflects overall protein dynamics. The rapid cooling of the crystal in liquid nitrogen traps various conformational states that can exist at 37 °C, although the thermodynamics of conformational changes may shift the equilibrium among states.[44,45] In this study, four different subunits were modeled, providing an opportunity to confirm assignments and to identify consistent conformations. As illustrated in Figure 2, Leu-57 and Leu-309 have alternative conformations in each structure, and Leu-116 has different conformations depending upon which alcohol is bound. Altogether, alternative conformations were modeled for 50 amino acid residues of the 748 in the dimeric molecule of each complex (Table 2). Approximately half of these residues are found in both subunits, indicating similar environments. Because the asymmetric unit is the dimeric molecule, the subunits can be different, but the structures of the subunits are almost identical. Four residues differ in their alternative conformations between the two structures. We can expect that other alternative conformations are present, but have not yet been identified, because fitting of electron density maps is never finished.

As expected, the longer chain amino acids (glutamine, glutamate, and lysine) on the surface have some propensity for occupying different positions, typically in energetically reasonable conformations. In several cases, two conformations were identified and more may be present, but the electron densities were not sufficient to model every position. Some of the glutamate positions result from a 120° rotation around the CA−CB bond, putting the carboxylates in very different places. The ε-amino group of lysine often seems to occupy alternative positions. Some alternative positions are unusual. The minor (4%) position for Cys-A46 in the structure with PFB may result from the loss of some catalytic zinc and thus would represent artifactual, chemical heterogeneity. Such heterogeneity was not observed in the positions of the other three Cys-46 residues. Backbone carbonyl groups for Glu-107 and Lys-247 exhibit some "wobble" that was enclosed in an enlarged electron density, but the side chain positions were not affected. Glu-B366 has the whole residue in alternative positions. The origin of these alternative conformations is not obvious.

Several water molecules with partial occupancies interact with the partially occupied amino acid side chains. The occupancies of these waters were adjusted to reflect the

dx.doi.org/10.1021/bi300378n | *Biochemistry* 2012, 51, 4035−4048

Table 3. Distances (angstroms) for Ligand Binding in Complexes of ADH

structure	NAD C4N−ligand "C"[a]	Zn−ligand O	Ser-48 OG−ligand O
PFB[b]			
A subunit	3.36 ± 0.02	1.97 ± 0.01	2.48 ± 0.01
B subunit	3.36 ± 0.03	1.98 ± 0.01	2.52 ± 0.03
TFE[b]			
A subunit	3.43 ± 0.03	1.97 ± 0.01	2.48 ± 0.01
B subunit	3.42 ± 0.06	1.98 ± 0.01	2.47 ± 0.10
FAlc,[c] av of 4	3.40 ± 0.03*	1.96 ± 0.02*	2.52 ± 0.02*
1P1R, av of 4[d]	3.48 ± 0.09	2.15 ± 0.04*	2.72 ± 0.03*
3BTO, av of 4[e]	3.56 ± 0.03*	2.10 ± 0.04*	2.67 ± 0.04*

[a]The ligands and the atoms corresponding to the reactive carbon ("C") are pentafluorobenzyl alcohol (C7), trifluoroethanol (C1, labeled as C2 for ETF in the PDB file), *N*-1-methylhexylformamide (C1), and 3-butylthiolane 1-oxide (S6). [b]The distances and errors calculated with SHELXL. [c]The distances for the four values for the fluoroalcohols from the REFMAC refinements were averaged (av) and compared to the averages of the four distances for the complexes with methylhexylformamide and 3-butylthiolane 1-oxide, and the asterisks indicate that the differences relative to the complexes with fluoroalcohols were significant at the $p < 0.01$ level. [d]X-ray data for NADH and (*R*)-*N*-1-methylhexylformamide [$CH_3(CH_2)_4CH(CH_3)NHCHO$] ($K_i$ = 15 μM) complexed with ADH at 1.57 Å resolution.[66] [e]X-ray data for NADH and (1*S*,3*S*)-3-butylthiolane 1-oxide (K_i = 0.72 μM) complexed with ADH at 1.66 Å resolution.[37]

occupancies of the side chains, rather than to let the temperature factors account for the partial occupancies. Several water molecules (30 in common for the two structures) also have alternative positions, which were modeled as doubled atoms.

An interesting example of alternative positions for a side chain and a water is Lys-228, which interacts with the adenosine monophosphate portion of NAD (Figure 3). The ε-amino (NE) group can interact indirectly via a water molecule with O3′ of the adenosine ribose and a phosphate oxygen or directly with O3′ and indirectly via the water in the alternative position with the phosphate oxygen. The occupancies range from ∼50:50 in the B subunit to 80:20 in the A subunit. It appears that the varied conformations may modulate binding interactions by increasing the fluidity of the site. The role of Lys-228 has been studied. The K228R substitution moderately increases steady-state kinetic constants (e.g., K_d values for NAD^+ and NADH increase by 4−7-fold), and the guanidino group of Arg-228 displaces the water and is accommodated with small, local changes.[34,46] Larger, chemical modifications of Lys-228 substantially affect coenzyme binding and can result in large increases in catalytic activity.[6,47]

Recent studies suggest that enzymes exist in an ensemble of different conformational states, including alternative conformations of side chains, and these states have different catalytic activities.[48,49] If each of the 50 alternative amino acid conformations identified in this study is independent, then the ensemble could include 10^{15} different conformations! Although amino acid residues throughout the protein may contribute to the dynamics of the scaffold, we suggest that the different conformations of leucine residues 57 and 309 may be most directly relevant for catalysis. Indeed, the L57F substitution unmasked hydrogen tunneling and increased the catalytic efficiency on benzyl alcohol by 2.8-fold.[7,50] Perhaps the phenylalanine residue limits the conformational flexibility and helps to position the substrate for reaction. The contributions of many other residues remain to be investigated.

Geometry of Ligand Binding. The high-resolution structures provide significant details about the arrangement of ligands and bond distances that are relevant for the mechanism (Table 3). As analogues of the Michaelis complexes, the distances between C4N of NAD^+ and what would be the reactive carbon (-CH_2-) of the alcohol are 3.40 ± 0.04 Å for the structures with PFB and TFE, when the distances in the four subunits of the two structures are averaged. (The individual values from refinements with SHELXL are given for each structure, and the values for the four fluoroalcohols from the refinements with REFMAC were averaged for comparison to other structures refined similarly.) The distance of 3.40 Å is a typical van der Waals distance, and the geometry is appropriate for direct transfer of a hydride ion from the alcohol to C4N of NAD^+. The complexes appear to be ready to form a transition state, without significant rotation of the single bonds around the methylene carbon.

Two moderately high-resolution (2.0 Å) structures have been determined for mutated horse liver ADHs complexed with NAD^+ and TFE: F93W enzyme (PDB entry 1AXE[51]) and F93W/V203A enzyme (PDB entry 1A71[52]). The unit cell for the structure determined at 277 K (PDB entry 1AXE) is slightly larger than the cell determined at 100 K, and the coenzyme binding domains can be superimposed with an rmsd of 0.26 Å. Because one or two amino acids are substituted in the active site, some differences can be expected in ligand binding relative to that of the wild type or each mutated enzyme. It appears the nicotinamide ring and the TFE are positioned differently in the mutated enzymes. The distance between C1 of TFE and C4N of NAD^+ averages 3.16 Å in the mutated F93W ADH, whereas the C1−C4N distance is 3.54 Å in the doubly mutated F93W/V203A ADH. The difference is attributed to the V203A substitution and is considered to be a critical factor in the extent of quantum mechanical tunneling during hydride transfer.[19,52] In the wild-type enzyme, the distance is 3.43 ± 0.03 Å. In the complex with NAD^+ and TFE with (non-zinc) ADH from *Drosophila melanogaster*, the distance between C4N and C1 of TFE is 3.29 Å (PDB entry 1SBY).

The distances in the NAD^+−alcohol complexes can be compared to those in structures that are analogues of the NADH−aldehyde complex to characterize the changes that occur during the catalytic reaction. The distances between C4N of NADH and the atom that corresponds to the reducible C of the carbonyl group in the structures with methylhexylformamide (PDB entry 1P1R) or 3-butylthiolane 1-oxide (PDB entry 3BTO) average 3.53 or 3.57 Å (Table 3). This would be a reasonable distance for the ground-state structure for the Michaelis complex of NADH and a carbonyl compound. The complex with the formamide may be the closest model of the

Table 4. Bond Distances (angstroms) in Nicotinamide Rings

	structure	N1−C2	C2−C3	C3−C4	C4−C5	C5−C6	C6−N1	average deviation
1	PFB, A subunit[a]	1.365 ± 0.011	1.362 ± 0.012	1.441 ± 0.013	1.415 ± 0.014	1.358 ± 0.013	1.420 ± 0.012	0.012
2	PFB, B subunit[a]	1.375 ± 0.024	1.353 ± 0.033	1.443 ± 0.018	1.394 ± 0.034	1.352 ± 0.034	1.391 ± 0.015	0.026
3	TFE, A subunit[a]	1.378 ± 0.013	1.365 ± 0.014	1.416 ± 0.017	1.371 ± 0.016	1.371 ± 0.014	1.398 ± 0.014	0.015
4	TFE, B subunit[a]	1.384 ± 0.087	1.354 ± 0.128	1.408 ± 0.026	1.376 ± 0.123	1.365 ± 0.123	1.389 ± 0.026	0.086
5	weighted average of four subunits[a]	1.371 ± 0.008	1.363 ± 0.009	1.432 ± 0.009	1.396 ± 0.010	1.363 ± 0.009	1.404 ± 0.007	0.009
6	REFMAC, average[b]	1.37	1.35	1.43	1.38	1.36	1.38	0.018
7	NAJ[c]	1.346	1.391	1.398	1.384	1.379	1.347	0.005
8	LiNAD$^+$[d]	1.39	1.37	1.40	1.42	1.37	1.35	0.02
9	NAD(P)$^+$[e]	1.36	1.38	1.40	1.39	1.38	1.37	0.014
10	dihydronicotinamide[f]	1.38	1.32	1.51	1.53	1.32	1.43	0.012
11	NADH, as NAJ[g]	1.40	1.38	1.50	1.46	1.36	1.46	0.034
12	NADH in ADH[h]	1.40	1.35	1.48	1.47	1.41	1.40	0.031
13	NADPH[i]	1.38	1.38	1.49	1.48	1.38	1.42	0.026

[a]Bond distances and errors from refinement with SHELXL with no restraints on the bond distances and planarity for the coenzyme. [b]Average bond distances (of four subunits) from refinement of PFB and TFE structures with REFMAC with relaxed restraints (0.10 Å) on distances and no restraints on the planarity of the nicotinamide ring (note that protons were removed on N1A and phosphate AO2 to represent the coenzyme at neutral pH). [c]Neutron diffraction at 0.65 Å resolution with estimated errors of 0.005 Å.[64] [d]X-ray data at 1.09 Å with estimated average errors of 0.02 Å.[89] The distances are within 0.03 Å of those found for *N*-1-(2,6-dichlorobenzyl)-3-carbamidopyridinium iodide.[90] [e]Five structures of enzymes complexed with NAD$^+$ determined at 1.0−1.2 Å resolution (PDB entries 1ZJZ, 1SBY, 1T2D, 3JY0, and 2O23) and five structures with NADP$^+$ determined at 0.66−1.0 Å resolution (PDB entries 1US0, 3BCJ, 1PWM, 2J8T, and 1ZK4). These values are within 0.01 Å of the target values in the dictionary from REFMAC where the restraints usually are set at 0.02 Å. [f]*N*-Benzyl-1,4-dihydronicotinamide.[91] The nicotinamide ring is planar. [g]Average of eight subunits in complexes of ADH with NADH, refined as NAJ, and (*R*)-*N*-1-methylhexylformamide (1.57 Å resolution, PDB entry 1P1R[66]) or (1*S*,3*S*)-3-butylthiolane 1-oxide (1.66 Å resolution, PDB entry 3BTO[37]). [h]Four structures (1.0−1.2 Å, average of eight subunits) of zinc or cadmium horse liver ADH complexed with NADH and isobutyramide, dimethyl sulfoxide, or hydroxide partly adducted to the nicotinamide ring (PDB entries 1HET, 1HEU, 2JHG, and 1JHF).[20,21] [i]Five structures of NADPH in enzymes determined at 1.09−1.35 Å resolution; all nicotinamide rings were essentially planar (PDB entries 3DJJ, 1LQU, 1YNQ, 1HEJ, and 1KMS).

Michaelis complex with an aldehyde, whereas the complex with the thiolane oxide may resemble the complex with cyclohexanone, which is a good substrate. The difference in distances between the structures with the alcohols and the 3-butylthiolane 1-oxide is significant, even though the resolutions of the structures with NADH are not as high as those with NAD$^+$ and the fluoroalcohols.

The average distance in the complexes between the O of the fluoroalcohols and the catalytic zinc is 1.96 Å, which would be consistent with the binding of an alkoxide. For comparison, the distances between the zinc and the doubly bonded O atom in the complexes with NADH are 2.15 and 2.10 Å, which differ significantly from the distances for the fluoroalcohols. Transient kinetic studies of proton release during binding of trifluoroethanol suggest that the p*K* of the ternary complex is 4.6,[53] and the crystals were prepared at pH 7, making it reasonable to assume an alkoxide is present. Comparable pH dependence studies have not been conducted with pentafluorobenzyl alcohol, but the withdrawal of electrons by the five fluorine atoms is expected to facilitate deprotonation of the alcohol. Molecular dynamics simulations provide Zn−O distances of ∼2.0 Å for the complex with NAD$^+$ and benzyl alcohol, increasing to ∼2.2 Å in the complex with NADH and benzaldehyde.[14,54]

Microscopic p*K* values for the ionization of substrate alcohols are difficult to assign, as the alcohols participate in the hydrogen-bonded network linked to His-51,[33] but apparent p*K* values derived from the pH dependence of hydride transfer give a p*K* value of 6.4 for ethanol and benzyl alcohol oxidations at 25 °C.[55,56] The p*K* for water bound to the enzyme−NAD$^+$ complex is estimated to be 7.3,[53] and it is reasonable to assume that the p*K* values of the bound alcohols would be lower than 7.3, yielding the alkoxides in the complexes.

The average distance between the O of the fluoroalcohol and the hydroxyl group of Ser-48 is 2.48 ± 0.01 Å (SHELXL refinement), shorter than expected for a typical hydrogen bond and in the range expected for a low-barrier hydrogen bond, which may be important for catalysis in enzymes.[57] Thus, the fluoroalcohol and the hydroxyl group share the proton, and each O would have alkoxide character. The structural results corroborate the studies of solvent isotope effects for benzyl alcohol oxidation, which showed an inverse effect of 2-fold (faster in D_2O than in H_2O), consistent with a partial charge on the substrate oxygen of −0.3 in the transition state.[50,58,59] The corresponding distances in the complexes with aldehyde analogues are 2.69 ± 0.04 Å, significantly longer than in the alcohol complexes and typical of a normal hydrogen bond.

High-resolution structures (1.45−1.65 Å) of human liver alcohol dehydrogenase isoenzymes complexed with formamides show geometry similar to those for the horse enzyme, with average distances of 3.85 Å between the carbonyl carbon of the formamide and C4N of NAD in ADH1B1 and 3.43 Å in ADH1C2 (PDB entries 1U3U, 1U3V, and 1U3W).[60] Likewise, the average distance between the O of the formamide and the catalytic zinc is 2.22 Å, and the distance from the O to the hydroxyl group of Ser/Thr-48 is 2.61 Å. However, in these structures, the coenzyme was refined as NAD$^+$ and the nicotinamide rings are planar. Perhaps these structures resemble "abortive" complexes.

Identification of the Coenzyme. The horse liver ADH was crystallized with NAD$^+$ and the fluoroalcohol, and it could be assumed that the crystals would contain the oxidized nicotinamide ring because the fluoroalcohols are not substrates and would also strongly inhibit oxidation of methylpentanediol and adventitious alcohols in the solutions. However, microspectrophotometry led to the suggestion that crystals prepared

dx.doi.org/10.1021/bi300378n | *Biochemistry* 2012, 51, 4035−4048

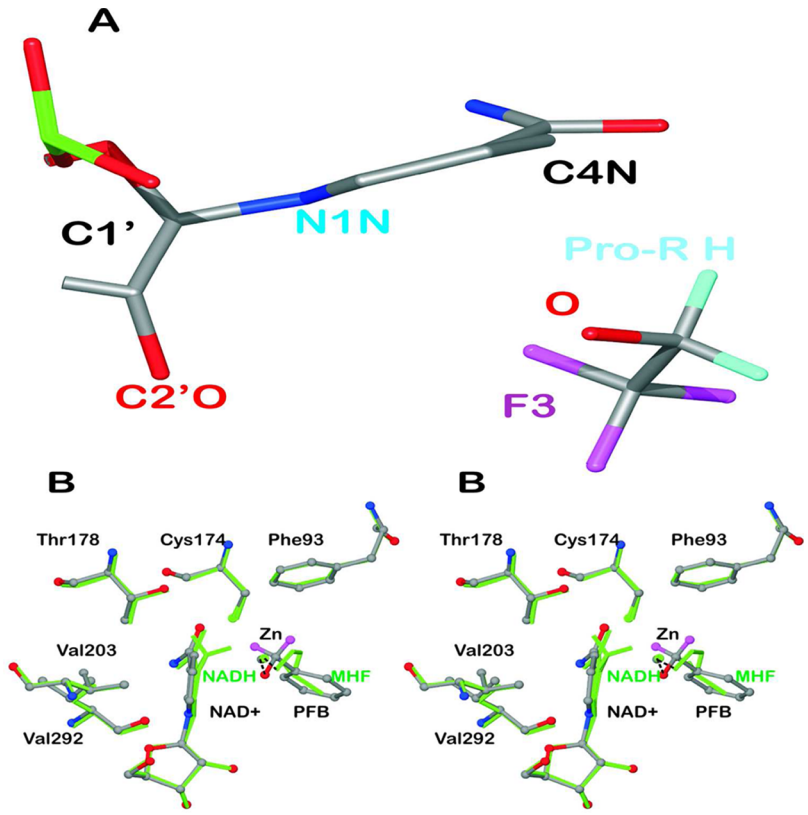

Figure 4. Puckering of the nicotinamide rings. (A) Structure of the complex with NAD^+ and TFE (subunit A) with atoms C2N and C3N aligned on top of atoms C5N and C6N so that the displacements of N1N and C4N from the plane are visible. (B) Comparison of the structure of the complex with NAD^+ and pentafluorobenzyl alcohol to that with NADH and methylhexylformamide. The "A" subunits of the structures (amino acid residues A1−A374) were superimposed, with an rmsd of 0.25 Å. The complex with NAD^+ and pentafluorobenzyl alcohol (with H atoms colored magenta but F atoms removed for the sake of clarity) is shown in atom coloring in a ball-and-stick representation. The complex with NADH (with H atoms on C4N) and methylhexylformamide (MHF, with atoms C3−C6 removed for the sake of clarity) is colored green. The residues making close contacts are labeled. The distances are listed in Table 5.

with NAD^+ and trifluoroethanol[61] contained 100% of the coenzyme as NADH.[62] We believe the formation of NADH in the crystals was an artifact due to washing of the crystals before spectrometry with a buffer containing only 30% methylpentanediol, which would reduce the NAD^+ when the inhibiting trifluoroethanol was removed. We found that mixing stoichiometric concentrations of enzyme and NAD^+ with excess methylpentanediol led to the substantial formation of NADH.[63] Note that our crystals were directly flash-cooled in liquid N_2 so that the NAD^+ and fluoroalcohol were still present. Nevertheless, the long time for crystallization (some weeks at 4 °C) and the possibility of radiation-induced reduction or damage of the nicotinamide ring require that the oxidation state of the coenzyme be assessed. The atomic-resolution data allow the structure of the coenzyme to be determined when we use a procedure appropriate for refinement of structures of enzymes crystallized with NAD^+ or NADH.

As described in Experimental Procedures, we used a modified dictionary for NAD in which the restraints on bond distances and ring planarity for the nicotinamide ring were relaxed, so that refinements could fit either NAD^+ or NADH. This molecule is named NAJ in our PDB entries, and it is based on the highest-resolution structure of NAD^+ available.[64] The results in Table 4 summarize the bond distances in the nicotinamide rings in various structures with oxidized and reduced nicotinamide rings. The first four rows of Table 4 present the results for the refinements with SHELXL. The bond distances in the nicotinamide rings for subunits A and B are the same within errors. The fifth row has the weighted average values from refinement of the PFB and TFE complexes, and the propagated errors are ∼0.01 Å for each distance. On the sixth row are the averages of the four distances from refinement with REFMAC. The bond distances determined by both refinement procedures are the same within the standard error of ∼0.02 Å, the same as the overall estimated coordinate error.

For comparison, Table 4 also gives the bond distances determined for the oxidized coenzyme (NAJ and LiNAD, rows 7 and 8) and averages for $NAD(P)^+$ in structures of 10 enzymes determined at a resolution better than 1.2 Å (row 9). Rows 10−13 contain experimental values for the reduced nicotinamide ring of a model compound as well as those from four structures of ADH with NADH or five structures with NADPH determined at high resolution (1.1−1.35 Å). The bond distances in the nicotinamide ring in the structures with the fluoroalcohols (row 5) most closely fit the distances determined for the oxidized coenzyme (row 9) rather than those for NAD(P)H (rows 10−13). In particular, the C3−C4 and C4−C5 bond distances in the complexes with the fluoroalcohols are shorter by 0.06−0.08 Å than those for the reduced nicotinamide rings. When the averaged values (four subunits) for the structures with pentafluorobenzyl alcohol and trifluoroethanol (row 5) are compared with those (eight subunits) for the structures of ADH complexed with NADH

dx.doi.org/10.1021/bi300378n | *Biochemistry* 2012, 51, 4035−4048

and carbonyl analogues (row 11, refined as NAJ), the differences are significant at the $p < 0.01$ level, and as compared to the values for NADPH (row 13), the differences are significant at the $p < 0.002$ level.

However, close examination shows some small but probably mechanistically significant differences in bond distances in the complexes. The C3−C4 bond distances for the nicotinamide rings in the complexes with fluoroalcohols are longer (compare rows 5 and 9) than those for NAD(P)$^+$ structures by ∼0.03 Å ($p < 0.03$), whereas the C4−C5 distance is not distinguishable from that in NAD(P)$^+$. Moreover, the C2−C3 bond distance is ∼0.02 Å shorter than the bonds in either NAD(P)$^+$ or NADPH ($p < 0.02$). The C5−C6 distance is ∼0.02 Å shorter than the bond in either NAD(P)$^+$ ($p < 0.01$) or NADPH ($p < 0.1$). The N1−C2 and C6−N1 bond distances are between (with differences of 0.01−0.03 Å) those for NAD(P)$^+$ ($p < 0.02$) and NADPH ($p < 0.3$). It does not appear that some mixture of NAD$^+$ and NADH is present in the complexes with the fluoroalcohols because the C4−C5 bond distance is the same as in the structures with oxidized nicotinamide rings. The electron density maps show no difference densities 2σ above the average in the $|F_o| - |F_c|$ maps. It was the plus/minus difference densities observed near C4N in the structures with NADH (PDB entry 1P1R) and NAD$^+$-pyrazole (PDB entry 1N8K) that led us to conclude that the nicotinamide rings were puckered and that the restraints in the refinement needed to be relaxed. As observed in Figure 1, the electron densities around C4N are similar to those for the other atoms in the ring, but the *B* factors for C4N are slightly higher (∼12%) than the average of the other five atoms in the ring. This indicates that the atoms are fitted well in density, but perhaps there is some loss of electron density or an increase in the level of motion at C4N. There is no evidence that the X-rays alter the state of oxidation of the coenzyme, as structures with either coenzyme are obtained. The observed structures are consistent with the hypothesis that the nicotinamide ring becomes slightly puckered with small alterations in bond distances and develops a partial positive charge on C4N in the transition state.[65]

Puckered Nicotinamide Rings. The structures with NAD$^+$ and fluoroalcohols have slightly puckered nicotinamide rings (quasi-boat conformation) with a torsion angle of 5.9 ± 1.5° (αC4[20]) for displacement of C4N in the C3−C4−C5 plane from the C2−C3−C6 plane and an angle of 4.8 ± 1.6° (αN1) for displacement of N1N in the N1−C2−C6 plane from the C2−C3−C6 plane as determined from the refinements of the four subunits with SHELXL (Figure 4A). These calculations account for the errors in atomic positions and a slight twist of the nicotinamide ring, but the C2−C3−C4−C5 torsion angle is the same within error. Nicotinamide rings of NADH have more obvious boat conformations, as demanded by the electron density maps and described for the first time for the complex of ADH with NADH and methylhexylformamide[66] (Figure 4B). The puckered rings (18° for αC4 and 12° for αN1 for PDB entry 1P1R) place C4N relatively closer to the carbonyl carbon of the substrate analogue, which may facilitate hydride transfer in reactive complexes.[14,54,67]

Previous structural analyses of enzymes that bind NAD(P) could have found puckered, oxidized nicotinamide rings; however, atomic resolution is required, and details of the refinement procedures and the state of oxidation are often not clear. Unfortunately, the default REFMAC dictionaries for oxidized and reduced NAD(P) enforce planarity for the nicotinamide rings, although bond distances are longer for the reduced ring. A systematic study of 340 PDB entries for structures containing NAD(P) determined at better than 2.0 Å resolution concluded that the structures with an oxidized nicotinamide ring, and even some with a reduced nicotinamide ring, were planar.[68] A small subset had distorted nicotinamide rings, and all of those with severe puckering (14 of them with torsion angles of >10°) had strong electrostatic interactions with oxygen atoms.[68] Some of these close contacts may be due to covalent adducts, as was described for NAD$^+$-pyrazole complexes with ADH, where the bond distances in the nicotinamide ring are close to those for NADH (refined as NAJ, PDB entries 1N92 and 1N8K).[69]

We surveyed the PDB for structures of enzymes with NAD(P)$^+$ determined at atomic resolution, which should yield good bond distances and perhaps evidence of ring puckering and close contacts. Five structures with NAD$^+$ have planar nicotinamide rings; four of five structures with NADP$^+$ have slightly puckered rings, and all have bond distances (Table 4, row 9) fitting those for NAJ and LiNAD (rows 7 and 8). All of the nicotinamide rings, except those described in PDB entries 1ZJZ, 3JYO, and 1ZK4, appear to have close contacts with oxygen atoms of the protein or a ligand. Good evidence of puckered, oxidized nicotinamide rings is sparse, except in the structures of ADH with fluorinated alcohols (including also PDB entry 3OQ6).

Structures with NAD(P)H may be expected to have puckered nicotinamide rings, as for two structures of ADH (Table 4, row 11). However, several structures with NADPH (Table 4, row 13) all have essentially planar rings, as does *N*-benzyldihydronicotinamide (row 10). Some structures have been reported with NADH, but the identification of the coenzyme and the refinement procedures are often not clear. A slightly puckered nicotinamide ring was refined for the abortive NADH/phenylalanine complex with L-phenylalanine dehydrogenase (PDB entry 1C1D, 1.25 Å), with bond distances most similar to those of reduced nicotinamide rings.[70] Somewhat puckered nicotinamide rings were described for the abortive NADH/UDP−glucose complex of UDP-galactose 4-epimerase (PDB entry 1EK6, 1.5 Å[71]) and for the NADH complex with aminoadipate semialdehyde dehydrogenase (PDB entry 2J6L, 1.3 Å), but the bond distances in the nicotinamide rings are closer to those for NAD$^+$ than for NADH. The abortive NADH/*R*-phenylethanol complex with the *R*-specific alcohol dehydrogenase (PDB entry 1ZJY, 1.05 Å) shows a planar nicotinamide ring with bond distances almost identical to those for NAD$^+$.[72] Some of these structures have close contacts with the nicotinamide rings, but their significance is not clear.

In contrast, atomic-resolution (1.0−1.2 Å) studies of several complexes of horse liver alcohol dehydrogenase with NADH, using refinements with relaxed restraints on the coenzyme, identified substantially puckered nicotinamide rings and bond distances that fit reduced nicotinamide rings (Table 4, row 12).[20,21] However, the interpretations of the electron density maps are complicated because of the evidence of covalent adducts with the nicotinamide rings, which produce a mixture of NADH forms in each active site. In one structure (PDB entry 1HET), 60% of the molecules apparently have a hydrated nicotinamide ring ("hydroxide" adduct, but the covalent bond distance is somewhat long at 1.96 Å), and the other 40% have the water in an alternative position that is typically occupied by the oxygen of the substrate analogues ligated to the catalytic zinc. The hydroxide adduct is suggested to activate the nicotinamide ring for hydride transfer and to participate as a

base in alcohol oxidation in a proposed central complex with a pentacoordinated zinc.[20] However, there is no good chemical rationale for this mechanism, and there is little room to accommodate five ligands on the zinc without some structurally significant rearrangements.[33] Moreover, in another structure (PDB entry 2JHG), with NADH and isobutyramide (an inhibitory analogue of a carbonyl substrate), the extra water is totally excluded, but adducts (with a bond distance of 1.95 Å) have apparently formed between the amino group of the amide and C4N of the nicotinamide with partial occupancy.[21] Hydroxide adducts with NADH were also proposed for complexes of ADH in which the catalytic zinc was replaced with Cd^{2+}.[20,21] Because of the heterogeneity of the complexes with adducts of NADH in each active site, it is not clear from these studies which structures are relevant for the catalytic mechanism.

Strained Nicotinamide Rings. Considering the slight puckering of the nicotinamide ring observed in the structures with fluoroalcohols (REFMAC or SHELXL refinements) and the altered bond distances as compared to those of oxidized nicotinamide rings, we suggest that the complexes represent a strained, oxidized ring part way on the path to the transition state. Although the statistical analyses are consistent with altered bond distances, the overall pattern of changes is illuminating as they are very similar to the differences calculated for the transition-state structure as compared to ground-state NAD^+ and NADH for formate dehydrogenase,[65] as discussed below.

Examination of the environment of the nicotinamide ring suggests that some close contacts may be responsible for the ring puckering. Figure 4B can illustrate the ground-state structures for the substrates and products. The nicotinamide ring in the complexes formed with NAD^+ and fluoroalcohols is slightly puckered (Figure 4A) and becomes more obviously puckered in complexes with NADH and carbonyl compounds. We suggest that close contacts with the protein may stress the nicotinamide ring in the oxidized state, and the stress is relieved in the reduced ring, which is obviously puckered, as could be expected from the tetrahedral bonding at C4N. Table 5 lists these contacts along with the corresponding distances in the structure with NADH and methylhexylformamide. The distances from atoms of the reduced ring to Cys-174 SG, Thr-178 CG2, and Val-292 O are significantly longer (0.05–0.20 Å) than those distances in the NAD^+–fluoroalcohol complexes. The puckering of the reduced nicotinamide ring observed in the structures with methylhexylformamide and 3-butylthiolane oxide (PDB entries 1P1R and 3BTO, respectively) moves C4N ~0.25 Å closer, as compared to the position with NAD^+, to the atom of the carbonyl analogue that would accept the hydride.

Table 5. Close Interactions of the Nicotinamide Rings in Complexes with ADH

contact to NAD(H)	NAD^+–fluoroalcohol	NADH, PDB entry 1P1R
Cys-174 SG–C4N	3.52 ± 0.01[a]	3.62 ± 0.04
Thr-178 OG1–C4N	3.42 ± 0.02	3.52 ± 0.04
Thr-178 CG2–C4N	3.39 ± 0.02[a]	3.59 ± 0.06[a]
Val-292 O–C2N	3.03 ± 0.01[a]	3.08 ± 0.02[a]
Val-203 CG2–C6N	3.64 ± 0.05	3.70 ± 0.05
Lig-378 O–C5N	3.04 ± 0.03[a]	3.21 ± 0.04[a]
Val-292 O–N7N	2.95 ± 0.02	2.98 ± 0.02
Ala-317 O–N7N	2.98 ± 0.02	2.97 ± 0.02
Phe-319 NH–O7N	2.85 ± 0.03	2.80 ± 0.04

[a]The differences between the average distances in the four subunits of complexes with the fluoroalcohols and methylhexylformamide are significant at the $p < 0.02$ level.

If the contacts observed between the enzyme and the oxidized coenzyme are contributing to the ring strain, substitution of the amino acid residues should affect catalytic activity. Indeed, the T178S substitution (loss of the CG2 methyl group contact) decreases the observed rate constant for hydride transfer with benzyl alcohol from 24 to 2.9 s^{-1} without affecting coenzyme binding, whereas the T178V substitution decreased the affinity for NADH and NAD^+ by 4- and 8-fold, respectively, without affecting hydride transfer.[69] The V203A substitution decreased the observed rate constant for hydride transfer to 1.5 s^{-1}. It is more difficult to probe the role of the carbonyl O of Val-292, but the V292A, -S, or -T substitution decreased the affinity for coenzymes 30–60-fold and the rate constant for hydride transfer to 5–9 s^{-1}. The isomerization of the V292S enzyme–NAD^+ complex (open conformation to closed) is hindered,[6,9] but the V292T enzyme forms a closed complex with the NAD^+-pyrazole adduct, which has a severely puckered nicotinamide ring that could resemble the transition state.[69] In these V292S or -T enzymes, a new water molecule that makes hydrogen bonds with the new hydroxyl group is inserted, but how this affects the conformational equilibrium is not clear. Via comparison of the structures of the wild-type and V292T enzymes complexed with NAD^+ and pyrazole (PDB entries 1N92 and 1N8K), the distances between C4N of the nicotinamide ring and Thr-178 OG1 and CG2 are ~0.07 Å longer in the mutated as compared to those of the wild-type enzyme, but the distances between Val-292 O and C2N are not affected. Although the alterations in rate constants and contact distances due to the amino acid substitutions are not very large, the experimental evidence of structural explanations is consistent with the suggestion that binding to the protein causes distortion of the nicotinamide ring in the ground state.

Mechanistic Conclusions. The atomic-resolution structures of the enzyme with NAD^+ and alcohols represent two different complexes that resemble the expected Michaelis complexes. We suggest that hydride would be transferred directly between the coenzyme and the substrate in an environment with a tetrahedral zinc after the proton from the alcohol is relayed through the hydrogen-bonded network to His-51 (Figure 1).[33,34] These structures complement those with NADH and analogues of the aldehyde substrate, particularly the one with methylhexylformamide, which resembles the Michaelis complex expected for the reverse reaction (Figure 4B). The geometry of the binding defines the distances for proton and hydride ion transfers. Each fluoroalcohol is formally deprotonated, but the alkoxide forms a low-barrier hydrogen bond to the Ser-48 OG hydroxyl group. Calculations show that the interaction of the alkoxide with zinc decreases the energy barrier for hydride transfer.[73] The distances between the O of the carbonyl analogues and Ser-48 OG and the zinc are significantly longer in the complexes mimicking the ADH–NADH–aldehyde complexes, consistent with calculations.[14] The interactions of the alcohols with the amino acid side chains determine that the *pro-R* hydrogen of the alcohol would be most directly transferred to the *re* face of the nicotinamide ring (Figure 2).

We do not think that any evidence supports a role for a water in activating the coenzyme in a central complex that would be

poised to transfer hydrogen.[20] A central, pentacoordinated complex with both the substrate oxygen and a water bound to the catalytic zinc was first proposed to explain NMR results,[74] but the idea was abandoned when the structure of a ternary complex showed no such coordination.[33] The various structures with water and substrate analogues in the same active site may be transient species that occur during replacement of the water ligated to the zinc by the oxygen of the substrate.[21] The exchange of water and substrate may occur via a pentacoordinate species or by a double-displacement mechanism involving Glu-68.[53]

The potential significance of the strained ground state for catalysis may be illustrated by comparing the equilibrium constant for the overall reaction (NAD^+ + alcohol ⇌ NADH + aldehyde) to the constant when the substrates are bound to the enzyme. At pH 7, the equilibrium constant (K_{eq}) for the oxidation of benzyl alcohol is 3.8×10^{-4} (favoring alcohol), whereas when the alcohol is bound to the enzyme, the "on-enzyme" equilibrium constant (K_{int}) is ~0.25.[63] Thus, it appears that the enzyme shifts the equilibrium position in favor of alcohol oxidation by a factor of 650, or 3.8 kcal/mol. Some of the intrinsic binding energy for NAD^+ may distort the nicotinamide ring, accounting for some of the shift. The positively charged nicotinamide ring also seems to shift the p*K* of the water bound to the catalytic zinc in the binary enzyme−NAD^+ complex by 2.2 units (3.0 kcal/mol).[53] If a similar shift occurs for alcohol bound to the zinc in the ternary complex, which would facilitate formation of the alkoxide, the distortion and p*K* shift could account for the shift in the equilibrium constant. At pH 7, the dissociation constant for NAD^+ is 120 μM and that for NADH is 0.41 μM.[63] If the intrinsic binding energy of NAD^+ is the same as that of NADH, some 3.4 kcal/mol is available to shift the on-enzyme equilibrium. (Some intrinsic binding energy is also used when the enzyme changes conformation, which may be approximately the same for both coenzymes.) The magnitudes of these energy changes are reasonable but are not definitively assigned to particular structural changes.

The on-enzyme equilibrium can also be affected by interactions of the enzyme with NADH and the aldehyde. Raman spectroscopy shows that the carbonyl group of a formamide is stabilized by 5.5 kcal/mol upon binding to ADH.[75] In contrast, a Raman study of the homologous lactate and malate dehydrogenases led to the suggestion that the binding NADH did not involve stabilization of the *pro-R* hydrogen in the binary complexes.[76] Further experimental and theoretical studies of ADH should determine the energetics of each step in the enzyme reaction.

As described in reviews of the role of strain in enzyme catalysis, the enzyme must bind, in principle, the transition state relatively more tightly than it binds the substrates and products.[77,78] If binding of substrates and the transition state were equally tight, the chemical reaction would occur no more rapidly in the presence of the enzyme than in the absence because the difference in energy between substrates and the transition state would be unchanged. Binding of the substrates may be less tight because some potential binding energy is used to destabilize the substrates, increasing the energy of the ground states and differentially lowering the barrier for the chemical step. Because the enzyme is not a rigid, or static, scaffold, the enzyme is also strained by the binding of substrates, and strain by itself could not account for all of the catalytic efficiency.

Computational analyses of the reaction of dehydrogenases have suggested that the nicotinamide ring is puckered in the transition state for hydride transfer, which would favorably position C4N of the nicotinamide ring for the transfer of hydride from an alcohol to the *re* face of the ring leading to a pseudoaxial orientation for the *pro-R* hydrogen in the reduced nicotinamide ring.[14,65,67,79−82] Distortion of the oxidized nicotinamide ring might also stabilize some carbonium ion character on C4N and facilitate the chemistry.[83] (The ^{15}N isotope effect of 1.0 for the N1N-labeled coenzyme on the reaction does not disprove the hypothesis, because bond order at N1N may not change significantly.[84]) Calculations for formate dehydrogenase show that deformation of the oxidized nicotinamide ring, to produce the quasi-boat structure of the proposed transition state, with puckering angles αC4 of 15° and αN1 of 5°, is estimated to require 16 kcal/mol, whereas similar puckering of the reduced nicotinamide ring requires only 1.5 kcal/mol and has a relatively flat free energy profile over the range from 20° to 30°.[67,85] The energy profile for deforming the oxidized nicotinamide ring has not been calculated.

Further calculations for the formate dehydrogenase reaction (gas phase or acetonitrile) characterized a transition-state structure for the coenzyme.[65] Relative to the oxidized ring in NAD^+, N1−C2 and C6−N1 bond distances increased by 0.02−0.03 in the transition state and 0.03−0.05 Å in the reduced ring. The C3−C4 and C4−C5 distances increased by 0.04−0.06 Å in the transition state and 0.11−0.14 Å in the final reduced ring of NADH. The C2−C3 and C5−C6 distances decreased in the transition state by 0.02−0.03 Å and decreased further to 0.04−0.05 Å in the reduced state. The changes in bond distances for the calculated transition states are very similar to those listed in Table 4 for NAD^+ in the complexes with the fluoroalcohols as compared to free NAD^+, except that the C3−C4 and C4−C5 distances are 0.03−0.05 Å shorter in the complexes than in the calculations. [We also note that the calculated changes in C2−C3 and C5−C6 distances in the reduced ring more closely match those in *N*-benzyldihydronicotinamide rather than in NAD(P)H as observed in the various enzyme complexes.] The αC4 puckering angle in the calculated transition state was 9° as compared to ~6° in the structures with fluoroalcohols. Of course, the crystallized enzyme complexes are not at the transition state, but the observed structures may define a strained state on the pathway to the transition state.

High-level, hybrid calculations that include all protein atoms and consider the quantum mechanical hydrogen tunneling provide important insights into the nature of the transition state. These calculations are validated by reproducing the free energy barrier for the transition state (15.5 kcal/mol for a rate constant for the transfer of hydride from benzyl alcohol of 38 s^{-1})[58] and the primary and secondary kinetic isotope effects that are evidence of the tunneling.[14,16,17] There are substantial motions in reaching the transition state, as the donor−acceptor distance between the reacting carbons decreases to ~2.6−2.7 Å. Many features of the enzyme contribute to the dynamics, but it was concluded that hydrophobic interactions, including those listed in Table 5, do not appreciably change the potential energy surface along the reaction path, whereas several polar residues (including Ser-48 and Asp-49) are important.[16,17] On the other hand, it appears that the steric interactions between Val-203 and Thr-178 with the nicotinamide ring affect the equilibrium free energy by promoting motions that change the donor−acceptor distance.[14,19] It appears that the complexes described here with the substrate analogues are beautifully

dx.doi.org/10.1021/bi300378n | *Biochemistry* 2012, 51, 4035−4048

"preorganized" [19] for hydride transfer, but what motions (reorganization) might be correlated with the chemical step need to be determined. Molecular dynamics and normal-mode analyses suggest that motions of domains (related to the global conformational change) could "push" the substrates together.[13,86] Equilibrium, vibrational motions might also be sufficient, however, as temperature factors of 10 Å^2 (observed in these structures, albeit at 100 K) could correspond to motions of 0.35 Å, leading to a decrease in the donor−acceptor distance from 3.4 to 2.7 Å. However, a recent, empirically parametrized model suggests that the "tunneling ready state" could have a donor−acceptor distance of 3.2 Å.[87] The atomic-resolution X-ray structures presented here resemble such a state and describe the scaffold and ensembles that can be relevant for further studies of the dynamics and catalysis.

■ ASSOCIATED CONTENT

Accession Codes

The X-ray coordinates and structure factors have been deposited in the Protein Data Bank as entries 4DWV for the enzyme complexed with NAD^+ and 2,3,4,5,6-pentafluorobenzyl alcohol and 4DXH for enzyme complexed with NAD^+ and 2,2,2-trifluoroethanol.

■ AUTHOR INFORMATION

Corresponding Author

*E-mail: bv-plapp@uiowa.edu. Phone: (319) 335-7909. Fax: (319) 335-9570.

Funding

This work was supported by U.S. Public Health Service, National Institutes of Health, Grants GM078446 and AA00279 to B.V.P.

Notes

The authors declare no competing financial interest.

■ ACKNOWLEDGMENTS

We thank Dr. Eric N. Brown for preliminary studies of the complex with trifluoroethanol, Dr. Lokesh Gakhar for assistance with the X-ray crystallography, and The University of Iowa Protein Crystallography Facility for instrumentation. Synchrotron data were collected at the Advanced Photon Source at Argonne National Laboratory. Results were obtained on beamline 23ID in the GM/CA-CAT, which has been funded in whole or in part with Federal funds from the National Cancer Institute (Y1-CO-1020) and the National Institute of General Medical Sciences (Y1-GM-1104). Use of the Advanced Photon Source was supported by the U.S. Department of Energy, Basic Energy Sciences, Office of Science, under Contract W-31-109-Eng-38. Results were also derived from work performed on beamline 19ID in the Structural Biology Center, with special assistance from Dr. Stephan Ginell. Argonne National Laboratory is operated by UChicago Argonne, LLC, for the U.S. Department of Energy, Office of Biological and Environmental Research, under Contract DE-AC02-06CH11357.

■ ABBREVIATIONS

ADH, alcohol dehydrogenase; PFB, 2,3,4,5,6-pentafluorobenzyl alcohol; TFE, 2,2,2-trifluoroethanol; rmsd, root-mean-square deviation.

■ REFERENCES

(1) Brändén, C.-I., Jörnvall, H., Eklund, H., and Furugren, B. (1975) Alcohol Dehydrogenases. In *The Enzymes*, 3rd ed., Vol. *11*, pp 103−190, Academic Press, San Diego.

(2) Pettersson, G. (1987) Liver alcohol dehydrogenase. *CRC Crit. Rev. Biochem. 21*, 349−389.

(3) Eklund, H., and Brändén, C.-I. (1987) Alcohol Dehydrogenase. In *Biological Macromolecules and Assemblies: Volume 3. Active Sites of Enzymes* (Jurnak, F. A., and McPherson, A., Eds.) pp 73−141, Wiley, New York.

(4) Eklund, H., and Ramaswamy, S. (2008) Medium- and short-chain dehydrogenase/reductase gene and protein families: Three-dimensional structures of MDR alcohol dehydrogenases. *Cell. Mol. Life Sci. 65*, 3907−3917.

(5) Brändén, C.-I., and Eklund, H. (1978) Coenzyme-induced conformational changes and substrate binding in liver alcohol dehydrogenase. *Ciba Found. Symp. 60*, 63−80.

(6) Plapp, B. V. (2010) Conformational changes and catalysis by alcohol dehydrogenase. *Arch. Biochem. Biophys. 493*, 3−12.

(7) Bahnson, B. J., Park, D.-H., Kim, K., Plapp, B. V., and Klinman, J. P. (1993) Unmasking of hydrogen tunneling in the horse liver alcohol dehydrogenase reaction by site-directed mutagenesis. *Biochemistry 32*, 5503−5507.

(8) Kohen, A., Cannio, R., Bartolucci, S., and Klinman, J. P. (1999) Enzyme dynamics and hydrogen tunnelling in a thermophilic alcohol dehydrogenase. *Nature 399*, 496−499.

(9) Rubach, J. K., Ramaswamy, S., and Plapp, B. V. (2001) Contributions of valine-292 in the nicotinamide binding site of liver alcohol dehydrogenase and dynamics to catalysis. *Biochemistry 40*, 12686−12694.

(10) Tsai, S., and Klinman, J. P. (2001) Probes of hydrogen tunneling with horse liver alcohol dehydrogenase at subzero temperatures. *Biochemistry 40*, 2303−2311.

(11) Mincer, J. S., and Schwartz, S. D. (2004) Rate-promoting vibrations and coupled hydrogen-electron transfer reactions in the condensed phase: A model for enzymatic catalysis. *J. Chem. Phys. 120*, 7755−7760.

(12) Caratzoulas, S., Mincer, J. S., and Schwartz, S. D. (2002) Identification of a protein-promoting vibration in the reaction catalyzed by horse liver alcohol dehydrogenase. *J. Am. Chem. Soc. 124*, 3270−3276.

(13) Luo, J., and Bruice, T. C. (2007) Low-frequency normal modes in horse liver alcohol dehydrogenase and motions of residues involved in the enzymatic reaction. *Biophys. Chem. 126*, 80−85.

(14) Billeter, S. R., Webb, S. P., Agarwal, P. K., Iordanov, T., and Hammes-Schiffer, S. (2001) Hydride transfer in liver alcohol dehydrogenase: Quantum dynamics, kinetic isotope effects, and role of enzyme motion. *J. Am. Chem. Soc. 123*, 11262−11272.

(15) Hammes-Schiffer, S. (2002) Impact of enzyme motion on activity. *Biochemistry 41*, 13335−13343.

(16) Cui, Q., Elstner, M., and Karplus, M. (2002) A theoretical analysis of the proton and hydride transfer in liver alcohol dehydrogenase (LADH). *J. Phys. Chem. B 106*, 2721−2740.

(17) Alhambra, C., Corchado, J., Sanchez, M. L., Garcia-Viloca, M., Gao, J., and Truhlar, D. G. (2001) Canonical variational theory for enzyme kinetics with the protein mean force and multidimensional quantum mechanical tunneling dynamics. Theory and application to liver alcohol dehydrogenase. *J. Phys. Chem. B 105*, 11326−11340.

(18) Villà, J., and Warshel, A. (2001) Energetics and dynamics of enzymatic reactions. *J. Phys. Chem. B 105*, 7887−7907.

(19) Nagel, Z. D., and Klinman, J. P. (2010) Update 1 of: Tunneling and dynamics in enzymatic hydride transfer. *Chem. Rev. 110*, PR41−PR67.

(20) Meijers, R., Morris, R. J., Adolph, H. W., Merli, A., Lamzin, V. S., and Cedergren-Zeppezauer, E. S. (2001) On the enzymatic activation of NADH. *J. Biol. Chem. 276*, 9316−9321.

(21) Meijers, R., Adolph, H. W., Dauter, Z., Wilson, K. S., Lamzin, V. S., and Cedergren-Zeppezauer, E. S. (2007) Structural evidence for a

ligand coordination switch in liver alcohol dehydrogenase. *Biochemistry 46*, 5446−5454.
(22) Dauter, Z. (2003) Protein structures at atomic resolution. *Methods Enzymol. 368*, 288−337.
(23) Ramaswamy, S., Eklund, H., and Plapp, B. V. (1994) Structures of horse liver alcohol dehydrogenase complexed with NAD^+ and substituted benzyl alcohols. *Biochemistry 33*, 5230−5237.
(24) Pflugrath, J. W. (1999) The finer things in X-ray diffraction data collection. *Acta Crystallogr. D55*, 1718−1725.
(25) Winn, M. D., Ballard, C. C., Cowtan, K. D., Dodson, E. J., Emsley, P., Evans, P. R., Keegan, R. M., Krissinel, E. B., Leslie, A. G., McCoy, A., McNicholas, S. J., Murshudov, G. N., Pannu, N. S., Potterton, E. A., Powell, H. R., Read, R. J., Vagin, A., and Wilson, K. S. (2011) Overview of the CCP4 suite and current developments. *Acta Crystallogr. D67*, 235−242.
(26) Jones, T. A., Zou, J.-Y., Cowan, S. W., and Kjeldgaard, M. (1991) Improved methods for building protein models in electron density maps and the location of errors in these models. *Acta Crystallogr. A47* (Part 2), 110−119.
(27) Sheldrick, G. M. (2008) A short history of SHELX. *Acta Crystallogr. A64*, 112−122.
(28) Laskowski, R. A., MacArthur, M. W., Moss, D. S., and Thornton, J. M. (1993) PROCHECK: A program to check the stereochemical quality of protein structures. *J. Appl. Crystallogr. 26*, 286−290.
(29) Frauenfelder, H., Hartmann, H., Karplus, M., Kuntz, I. D., Jr., Kuriyan, J., Parak, F., Petsko, G. A., Ringe, D., Tilton, R. F., Jr., Connolly, M. L., and Max, N. (1987) Thermal expansion of a protein. *Biochemistry 26*, 254−261.
(30) Tilton, R. F., Jr., Dewan, J. C., and Petsko, G. A. (1992) Effects of temperature on protein structure and dynamics: X-ray crystallographic studies of the protein ribonuclease-A at nine different temperatures from 98 to 320 K. *Biochemistry 31*, 2469−2481.
(31) Kurinov, I. V., and Harrison, R. W. (1995) The influence of temperature on lysozyme crystals. Structure and dynamics of protein and water. *Acta Crystallogr. D51*, 98−109.
(32) Herdendorf, T. J., and Plapp, B. V. (2011) Origins of the high catalytic activity of human alcohol dehydrogenase 4 studied with horse liver A317C alcohol dehydrogenase. *Chem.-Biol. Interact. 191*, 42−47.
(33) Eklund, H., Plapp, B. V., Samama, J. P., and Brändén, C.-I. (1982) Binding of substrate in a ternary complex of horse liver alcohol dehydrogenase. *J. Biol. Chem. 257*, 14349−14358.
(34) LeBrun, L. A., Park, D.-H., Ramaswamy, S., and Plapp, B. V. (2004) Participation of histidine-51 in catalysis by horse liver alcohol dehydrogenase. *Biochemistry 43*, 3014−3026.
(35) Levy, H. R., and Vennesland, B. (1957) The stereospecificity of enzymatic hydrogen transfer from diphosphopyridine nucleotide. *J. Biol. Chem. 228*, 85−96.
(36) Green, D. W., Sun, H.-W., and Plapp, B. V. (1993) Inversion of the substrate specificity of yeast alcohol dehydrogenase. *J. Biol. Chem. 268*, 7792−7798.
(37) Cho, H., Ramaswamy, S., and Plapp, B. V. (1997) Flexibility of liver alcohol dehydrogenase in stereoselective binding of 3-butylthiolane 1-oxides. *Biochemistry 36*, 382−389.
(38) Ramaswamy, S., Scholze, M., and Plapp, B. V. (1997) Binding of formamides to liver alcohol dehydrogenase. *Biochemistry 36*, 3522−3527.
(39) Bondi, A. (1964) van der Waals volumes and radii. *J. Phys. Chem. 68*, 441−451.
(40) Nyburg, S. C., and Faerman, C. H. (1985) A revision of van der Waals atomic radii for molecular crystals: N, O, F, S, Cl, Se, Br and I bonded to carbon. *Acta Crystallogr. B41*, 274−279.
(41) Thalladi, V. R., Weiss, H. C., Blaser, D., Boese, R., Nangia, A., and Desiraju, G. R. (1998) C-H···F interactions in the crystal structures of some fluorobenzenes. *J. Am. Chem. Soc. 120*, 8702−8710.
(42) Kim, C. Y., Chang, J. S., Doyon, J. B., Baird, T. T., Jr., Fierke, C. A., Jain, A., and Christianson, D. W. (2000) Contribution of fluorine to protein-ligand affinity in the binding of fluoroaromatic inhibitors to carbonic anhydrase II. *J. Am. Chem. Soc. 122*, 12125−12134.
(43) Shapiro, S., Arunachalam, T., and Caspi, E. (1983) Equilibration of 1-octanol with alcohol dehydrogenase. Evidence for horse liver alcohol dehydrogenase responsibility for exchange of the 1-*pro-S* hydrogen atom. *J. Am. Chem. Soc. 105*, 1642−1646.
(44) Halle, B. (2004) Biomolecular cryocrystallography: Structural changes during flash-cooling. *Proc. Natl. Acad. Sci. U.S.A. 101*, 4793−4798.
(45) Fraser, J. S., Clarkson, M. W., Degnan, S. C., Erion, R., Kern, D., and Alber, T. (2009) Hidden alternative structures of proline isomerase essential for catalysis. *Nature 462*, 669−673.
(46) LeBrun, L. A., and Plapp, B. V. (1999) Control of coenzyme binding to horse liver alcohol dehydrogenase. *Biochemistry 38*, 12387−12393.
(47) Plapp, B. V. (1970) Enhancement of the activity of horse liver alcohol dehydrogenase by modification of amino groups at the active sites. *J. Biol. Chem. 245*, 1727−1735.
(48) Hammes, G. G., Benkovic, S. J., and Hammes-Schiffer, S. (2011) Flexibility, diversity, and cooperativity: Pillars of enzyme catalysis. *Biochemistry 50*, 10422−10430.
(49) Nagel, Z. D., Dong, M., Bahnson, B. J., and Klinman, J. P. (2011) Impaired protein conformational landscapes as revealed in anomalous Arrhenius prefactors. *Proc. Natl. Acad. Sci. U.S.A. 108*, 10520−10525.
(50) Plapp, B. V. (2006) Catalysis by alcohol dehydrogenases. In *Isotope Effects in Chemistry and Biology* (Kohen, A., and Limbach, H. H., Eds.) pp 811−835, CRC Press, Taylor and Francis, Boca Raton, FL.
(51) Bahnson, B. J., Colby, T. D., Chin, J. K., Goldstein, B. M., and Klinman, J. P. (1997) A link between protein structure and enzyme catalyzed hydrogen tunneling. *Proc. Natl. Acad. Sci. U.S.A. 94*, 12797−12802.
(52) Colby, T. D., Bahnson, B. J., Chin, J. K., Klinman, J. P., and Goldstein, B. M. (1998) Active site modifications in a double mutant of liver alcohol dehydrogenase: Structural studies of two enzyme-ligand complexes. *Biochemistry 37*, 9295−9304.
(53) Kovaleva, E. G., and Plapp, B. V. (2005) Deprotonation of the horse liver alcohol dehydrogenase-NAD^+ complex controls formation of the ternary complexes. *Biochemistry 44*, 12797−12808.
(54) Luo, J., and Bruice, T. C. (2001) Dynamic structures of horse liver alcohol dehydrogenase (HLADH): Results of molecular dynamics simulations of HLADH-NAD^+-$PhCH_2OH$, HLADH-NAD^+-$PhCH_2O^-$, and HLADH-NADH-PhCHO. *J. Am. Chem. Soc. 123*, 11952−11959.
(55) Brooks, R. L., Shore, J. D., and Gutfreund, H. (1972) The effects of pH and temperature on hydrogen transfer in the liver alcohol dehydrogenase mechanism. *J. Biol. Chem. 247*, 2382−2383.
(56) Kvassman, J., and Pettersson, G. (1978) Effect of pH on the process of ternary-complex interconversion in the liver-alcohol-dehydrogenase reaction. *Eur. J. Biochem. 87*, 417−427.
(57) Cleland, W. W., Frey, P. A., and Gerlt, J. A. (1998) The low barrier hydrogen bond in enzymatic catalysis. *J. Biol. Chem. 273*, 25529−25532.
(58) Sekhar, V. C., and Plapp, B. V. (1990) Rate constants for a mechanism including intermediates in the interconversion of ternary complexes by horse liver alcohol dehydrogenase. *Biochemistry 29*, 4289−4295.
(59) Ramaswamy, S., Park, D.-H., and Plapp, B. V. (1999) Substitutions in a flexible loop of horse liver alcohol dehydrogenase hinder the conformational change and unmask hydrogen transfer. *Biochemistry 38*, 13951−13959.
(60) Gibbons, B. J., and Hurley, T. D. (2004) Structure of three class I human alcohol dehydrogenases complexed with isoenzyme specific formamide inhibitors. *Biochemistry 43*, 12555−12562.
(61) Plapp, B. V., Eklund, H., and Brändén, C.-I. (1978) Crystallography of liver alcohol dehydrogenase complexed with substrates. *J. Mol. Biol. 122*, 23−32.
(62) Bignetti, E., Rossi, G. L., and Zeppezauer, E. (1979) Microspectrophotometric measurements on single crystals of

coenzyme containing complexes of horse liver alcohol dehydrogenase. *FEBS Lett. 100*, 17−22.
(63) Shearer, G. L., Kim, K., Lee, K. M., Wang, C. K., and Plapp, B. V. (1993) Alternative pathways and reactions of benzyl alcohol and benzaldehyde with horse liver alcohol dehydrogenase. *Biochemistry 32*, 11186−11194.
(64) Guillot, B., Lecomte, C., Cousson, A., Scherf, C., and Jelsch, C. (2001) High-resolution neutron structure of nicotinamide adenine dinucleotide. *Acta Crystallogr. D57*, 981−989.
(65) Schiøtt, B., Zheng, Y. J., and Bruice, T. C. (1998) Theoretical investigation of the hydride transfer from formate to NAD^+ and the implications for the catalytic mechanism of formate dehydrogenase. *J. Am. Chem. Soc. 120*, 7192−7200.
(66) Venkataramaiah, T. H., and Plapp, B. V. (2003) Formamides mimic aldehydes and inhibit liver alcohol dehydrogenases and ethanol metabolism. *J. Biol. Chem. 278*, 36699−36706.
(67) Almarsson, Ö., and Bruice, T. C. (1993) Evaluation of the factors influencing reactivity and stereospecificity in NAD(P)H dependent dehydrogenase enzymes. *J. Am. Chem. Soc. 115*, 2125−2138.
(68) Meijers, R., and Cedergren-Zeppezauer, E. (2009) A variety of electrostatic interactions and adducts can activate NAD(P) cofactors for hydride transfer. *Chem.-Biol. Interact. 178*, 24−28.
(69) Rubach, J. K., and Plapp, B. V. (2003) Amino acid residues in the nicotinamide binding site contribute to catalysis by horse liver alcohol dehydrogenase. *Biochemistry 42*, 2907−2915.
(70) Brunhuber, N. M. W., Thoden, J. B., Blanchard, J. S., and Vanhooke, J. L. (2000) *Rhodococcus* L-phenylalanine dehydrogenase: Kinetics, mechanism, and structural basis for catalytic specifity. *Biochemistry 39*, 9174−9187.
(71) Thoden, J. B., Wohlers, T. M., Fridovich-Keil, J. L., and Holden, H. M. (2000) Crystallographic evidence for Tyr 157 functioning as the active site base in human UDP-galactose 4-epimerase. *Biochemistry 39*, 5691−5701.
(72) Schlieben, N. H., Niefind, K., Muller, J., Riebel, B., Hummel, W., and Schomburg, D. (2005) Atomic resolution structures of *R*-specific alcohol dehydrogenase from *Lactobacillus brevis* provide the structural bases of its substrate and cosubstrate specificity. *J. Mol. Biol. 349*, 801−813.
(73) Agarwal, P. K., Webb, S. P., and Hammes-Schiffer, S. (2000) Computational studies of the mechanism for proton and hydride transfer in liver alcohol dehydrogenase. *J. Am. Chem. Soc. 122*, 4803−4812.
(74) Dworschack, R. T., and Plapp, B. V. (1977) pH, isotope, and substituent effects on the interconversion of aromatic substrates catalyzed by hydroxybutyrimidylated liver alcohol dehydrogenase. *Biochemistry 16*, 2716−2725.
(75) Deng, H., Schindler, J. F., Berst, K. B., Plapp, B. V., and Callender, R. (1998) A Raman spectroscopic characterization of bonding in the complex of horse liver alcohol dehydrogenase with NADH and *N*-cyclohexylformamide. *Biochemistry 37*, 14267−14278.
(76) Deng, H., Zheng, J., Sloan, D., Burgner, J., and Callender, R. (1992) A vibrational analysis of the catalytically important C4-H bonds of NADH bound to lactate or malate dehydrogenase: Ground state effects. *Biochemistry 31*, 5085−5092.
(77) Jencks, W. P. (1986) *Catalysis in Chemistry and Enzymology*, Dover, New York.
(78) Hackney, D. D. (1990) Binding energy and catalysis. In *The Enzymes* (Sigman, D. S., and Boyer, P. D., Eds.) 3rd ed., pp 1−36, Academic Press, San Diego.
(79) Tapia, O., Cardenas, R., Andres, J., and Colonna-Cesari, F. (1988) Transition structure for hydride transfer to pyridinium cation from methanolate: Modeling of LADH catalyzed reaction. *J. Am. Chem. Soc. 110*, 4046−4047.
(80) Wu, Y. D., and Houk, K. N. (1991) Theoretical evaluation of conformational preferences of NAD^+ and NADH: An approach to understanding the stereospecificity of NAD^+ NADH-dependent dehydrogenases. *J. Am. Chem. Soc. 113*, 2353−2358.
(81) Almarsson, Ö., Karaman, R., and Bruice, T. C. (1992) Kinetic importance of conformations of nicotinamide adenine dinucleotide in the reactions of dehydrogenase enzymes. *J. Am. Chem. Soc. 114*, 8702−8704.
(82) Webb, S. P., Agarwal, P. K., and Hammes-Schiffer, S. (2000) Combining electronic structure methods with the calculation of hydrogen vibrational wavefunctions: Application to hydride transfer in liver alcohol dehydrogenase. *J. Phys. Chem. B 104*, 8884−8894.
(83) Cook, P. F., Oppenheimer, N. J., and Cleland, W. W. (1981) Secondary deuterium and nitrogen-15 isotope effects in enzyme-catalyzed reactions. Chemical mechanism of liver alcohol dehydrogenase. *Biochemistry 20*, 1817−1825.
(84) Rotberg, N. S., and Cleland, W. W. (1991) Secondary ^{15}N isotope effects on the reactions catalyzed by alcohol and formate dehydrogenases. *Biochemistry 30*, 4068−4071.
(85) Young, L., and Post, C. B. (1993) Free-energy calculations involving internal coordinate constraints to determine puckering of a 6-membered ring molecule. *J. Am. Chem. Soc. 115*, 1964−1970.
(86) Luo, J., and Bruice, T. C. (2004) Anticorrelated motions as a driving force in enzyme catalysis: The dehydrogenase reaction. *Proc. Natl. Acad. Sci. U.S.A. 101*, 13152−13156.
(87) Roston, D., and Kohen, A. (2010) Elusive transition state of alcohol dehydrogenase unveiled. *Proc. Natl. Acad. Sci. U.S.A. 107*, 9572−9577.
(88) Brunger, A. T. (1992) Free R-value: A novel statistical quantity for assessing the accuracy of crystal structures. *Nature 355*, 472−475.
(89) Reddy, B. S., Saenger, W., Mühlegger, K., and Weimann, G. (1981) Crystal and molecular structure of the lithium salt of nicotinamide adenine dinucleotide dihydrate (NAD^+, DPN^+, Cozymase, Codehydrase I). *J. Am. Chem. Soc. 103*, 907−914.
(90) Brändén, C.-I., Lindqvist, I., and Zeppezauer, M. (1968) Model compounds for NAD-reactions: I. The crystal structure of *N*-1-(2,6-dichlorobenzyl)-3-carbamidopyridinium iodide monohydrate. *Ark. Kemi 30*, 41−50.
(91) Karle, I. L. (1961) Crystal structure of *N*-benzyl-1,4-dihydronicotinamide. *Acta Crystallogr. 14*, 497−502.